

## Excitation functions of threshold reactions on $^{45}\text{Sc}$ and $^{55}\text{Mn}$ induced by 6 to 13 MeV neutrons

M. Bostan\* and S. M. Qaim

*Institut für Nuklearchemie, Forschungszentrum Jülich GmbH, D-52425 Jülich, Federal Republic of Germany*

(Received 24 August 1993)

Excitation functions were measured for the  $^{45}\text{Sc}(n,2n)^{44}\text{Sc}^m$ ,  $^{45}\text{Sc}(n,2n)^{44}\text{Sc}^{m+g}$ , and  $^{55}\text{Mn}(n,2n)^{54}\text{Mn}$  reactions from threshold to 13 MeV, and for the  $^{45}\text{Sc}(n,p)^{45}\text{Ca}$ ,  $^{45}\text{Sc}(n,\alpha)^{42}\text{K}$ ,  $^{55}\text{Mn}(n,p)^{55}\text{Cr}$ , and  $^{55}\text{Mn}(n,\alpha)^{52}\text{V}$  reactions over the neutron energy range of 6 to 13 MeV. The quasimonoenergetic neutrons were produced via the  $^2\text{H}(d,n)^3\text{He}$  reaction using a deuterium gas target at a variable energy compact cyclotron. The activation technique in combination with high resolution  $\gamma$ -ray spectroscopy was used. In the case of the  $^{45}\text{Sc}(n,p)^{45}\text{Ca}$  and  $^{55}\text{Mn}(n,p)^{55}\text{Cr}$  reaction products, "low-level"  $\beta^-$  counting was applied. The reaction product  $^{45}\text{Ca}$  was separated radiochemically prior to  $\beta^-$  counting. Statistical model calculations taking into account precompound effects were performed for all the reactions studied. The experimental excitation functions are reproduced well by the calculation except for the  $(n,\alpha)$  reaction on the  $^{45}\text{Sc}$  target.

PACS number(s): 24.10.-i, 24.60.-k, 25.40.-h, 28.20.-v

### I. INTRODUCTION

Studies of excitation functions of neutron threshold reactions on medium and heavy mass nuclei are of considerable significance for testing nuclear models and for practical applications. The data are needed in fusion reactor technology (FRT) for calculations on nuclear heating, activation of reactor components, formation of hydrogen and helium gas in structural materials, radiation damage effects, etc. A survey of the available literature (cf. [1,2]) shows that cross section data for many neutron-induced reactions around threshold energies are rather scanty. We chose to investigate the neutron induced reactions on  $^{45}\text{Sc}$  and  $^{55}\text{Mn}$ . For both these target nuclei the cross section database below 13 MeV was very weak.

### II. EXPERIMENTAL

The experimental techniques used were similar to those described in several publications from this Institute (cf. [3-6]). Here we mention only some salient features relevant to the present measurements.

#### A. Neutron irradiations and background corrections

One gram of high-purity  $\text{Sc}_2\text{O}_3$  or  $\text{MnO}_2$  powder (> 99.9%) was pressed to obtain a pellet of 1.3 cm diam and 0.35 cm thickness by means of an electrohydraulic press. For studies on the  $^{55}\text{Mn}(n,p)^{55}\text{Cr}$  reaction, which leads to the pure  $\beta^-$  emitter  $^{55}\text{Cr}$ , 100 mg  $\text{MnO}_2$  powder was packed in a thin polyethylene bag. The moni-

tor foils (aluminum and iron, each 200  $\mu\text{m}$  thick) were attached at the front and the back of the sample. The samples were irradiated in the  $0^\circ$  direction relative to the deuteron beam with quasimonoenergetic neutrons produced via the  $^2\text{H}(d,n)^3\text{He}$  reaction on a  $\text{D}_2$  gas target at the variable energy compact cyclotron CV28. The characteristics of the neutron source are described in detail in Ref. [3]. The distance from the end of the gas target to the front face of the sample was 1.0 cm. In general, the irradiation time was approximately 2 h, in the case of  $^{55}\text{Mn}(n,\alpha)^{52}\text{V}$  and  $^{55}\text{Mn}(n,p)^{55}\text{Cr}$  reactions, however, due to the short half-lives of the products, the irradiation time was 10 min.

The primary deuteron energy was varied between 4.0 and 10.0 MeV to produce quasimonoenergetic neutrons in the energy range 6.30-12.85 MeV. At each energy two different irradiations (gas in/out) were performed (cf. [3]) to determine the contribution of background neutrons other than those due to breakup of deuterons on the  $\text{D}_2$  gas. The contribution from the background neutrons to the total activity is appreciable at deuteron energies higher than 7 MeV, especially when the reaction threshold is low, such as in the case of  $(n,\alpha)$  and  $(n,p)$  reactions. As far as the contribution from breakup neutrons was concerned, we used results of Cabral *et al.* [7]. By interpolating the values supplied by those authors at different neutron energies for reactions of different thresholds, we obtained the ratio of breakup to  $(d,n)$  neutron yields over the deuteron energy range 6-10 MeV.

#### B. Measurement of neutron flux density

The neutron flux density was determined via the monitor reaction  $^{56}\text{Fe}(n,p)^{56}\text{Mn}$  ( $T_{1/2} = 2.58$  h;  $E_\gamma = 847$  keV;  $I_\gamma = 98.87\%$ ) over the neutron energy region between 6.0 and 8.0 MeV and the  $^{27}\text{Al}(n,\alpha)^{24}\text{Na}$  ( $T_{1/2} = 15.0$  h;  $E_\gamma = 1368$  keV;  $I_\gamma = 100\%$ ) reaction between 8.0

\*Permanent address: Physics Department, Çekmece Nuclear Research and Training Center, 34622 Istanbul, Turkey.

and 13.0 MeV. The cross sections of both the monitor reactions were taken from Ref. [8]. The mean neutron flux densities ranged between  $1.10 \times 10^7$  and  $3.0 \times 10^7$   $\text{cm}^{-2} \text{s}^{-1}$ . The average neutron energy effective at the sample was calculated by a small Monte Carlo program (cf. [4,9]). The energy of the neutrons (as well as of the incident deuterons) was checked via a set of monitor reactions having different reaction thresholds (cf. [10]).

### C. Radiochemical separation of $^{45}\text{Ca}$

The irradiated  $\text{Sc}_2\text{O}_3$  sample was dissolved in HCl and  $\text{CaCl}_2$  carrier added to it. On neutralization,  $\text{Sc}(\text{OH})_3$  was precipitated and centrifuged off. Thereafter calcium was precipitated as oxalate. After several purification cycles the oxalate was converted to  $\text{CaCO}_3$  by heating at 500 °C, transferred to an Al planchet and fixed with glue. The chemical yield was approximately 80% and the uncertainty about  $\pm 3\%$ . Other details relevant to  $\beta^-$  counting were the same as described earlier [6].

### D. Measurement of radioactivity

The radioactivity of most of the reaction products was determined via Ge(Li) or HPGe detector  $\gamma$ -ray spectroscopy. Low-level  $\beta^-$  counting was applied for  $^{45}\text{Ca}$  and  $^{55}\text{Cr}$ . In the case of  $^{55}\text{Cr}$  the  $\beta^-$  end point energy is 2.5 MeV and so the thin  $\text{MnO}_2$  irradiated sample could be counted without a chemical separation. On the other hand, since  $^{52}\text{V}$ , the product of  $(n, \alpha)$  reaction on  $^{55}\text{Mn}$ , has the same half-life and  $\beta^-$  end point energy as  $^{55}\text{Cr}$ , it was mandatory to subtract the contribution of  $^{52}\text{V}$  from the total  $\beta^-$  activity. This did not cause any problem since the activity of  $^{52}\text{V}$  could be determined independently via  $\gamma$ -ray spectroscopy. In the case of  $^{45}\text{Ca}$  ( $E_{\beta^-} = 258$  keV) a chemically separated thin sample (see above) was used for  $\beta^-$  counting.

The activities of the reaction products were corrected for contributions from background neutrons (gas in/out results, breakup neutron contribution). From the cor-

rected count rates, the decay rates were obtained using the  $\beta^-$  or  $\gamma$ -ray emission probability and the efficiency of the detector. The decay data used for the reaction products were taken from Ref. [11] and are given in Table I.

### E. Calculation of cross sections and errors

Cross sections were calculated using the well-known activation equation. The principal sources of errors and their magnitudes involved in the two types of measurements are given in Table II. The individual errors were combined in quadrature to obtain the total error for each cross section value.

## III. NUCLEAR MODEL CALCULATIONS

Calculations were performed in the framework of the statistical model, utilizing the exciton model formalism for preequilibrium particle emission, the width-fluctuation corrected Hauser-Feshbach formula for first chance emission from the equilibrated system, and the evaporation formula for higher chance emission. The computer code STAPRE was used [12]. The particle transmission coefficients used in the calculations were derived from the spherical optical model, using global optical potentials given by Rapaport *et al.* [13] for neutrons, Perey and Buck [14] for protons, and McFadden and Satchler [15] for alpha particles. The internal transition rates were calculated according to the formulas by Williams [16]. A value of 135 as the constant in the squared matrix element for internal transitions was used [17]. For the  $\alpha$ -preformation parameter a value of 0.30 was taken [18]. In the product nuclei, the excited states up to about 5 MeV were taken from the Nuclear Data Sheets [19]; those above the region of discrete levels were treated as a continuum described by the back-shifted Fermi gas model. The choice of the level density parameters was guided by the compilation of Dilg *et al.* [20]. In the back-shifted Fermi gas model, the formula with shifted ground state was adopted, and both the fictive ground-state position

TABLE I. Decay data of reaction products studied.

Nuclear reaction	Q value <sup>a</sup> (MeV)	Half-life <sup>b</sup> of product	$E_\gamma$ <sup>b</sup> (keV)	$I_\gamma$ <sup>b</sup> (%)
$^{45}\text{Sc}(n, 2n)^{44}\text{Sc}^g$	-11.31	3.93 h	1157.0	99.9
$^{45}\text{Sc}(n, 2n)^{44}\text{Sc}^m$	-11.58	2.44 d	271.2	86.6
$^{45}\text{Sc}(n, \alpha)^{42}\text{K}$	-0.40	12.36 h	1524.6	18.8
$^{45}\text{Sc}(n, p)^{45}\text{Ca}$	-0.54	163.80 d	$E_{\beta^-} = 258$ keV	$I_{\beta^-} = 100$
$^{55}\text{Mn}(n, 2n)^{54}\text{Mn}$	-10.41	312.2 d	834.8	99.98
$^{55}\text{Mn}(n, \alpha)^{52}\text{V}$	-0.62	3.7 min	1434.1	100.0
$^{55}\text{Mn}(n, p)^{55}\text{Cr}$	-1.82	3.5 min	$E_{\beta^-} = 2500$ keV	$I_{\beta^-} = 100$

<sup>a</sup>Calculated using the mass excess given in Ref. [11].

<sup>b</sup>Taken from Ref. [11].

TABLE II. Principal sources of errors and their magnitudes.

Source of uncertainty	Magnitude%		
	Gamma counting ( $n, 2n$ )	( $n, \alpha$ )	Beta counting ( $n, p$ )
<i>Uncorrelated</i>			
Sample weight	0.1	0.1	0.1
Irradiation time	0.1	0.1	0.1
Irradiation geometry and beam deviation	3	3	3
Error in peak area analysis	3	3	
Statistics of counting	3	3	3
Chemical yield <sup>a</sup>			3
Correction for activity induced by background neutrons (gas in/out, breakup)	1-3	5-20 <sup>b</sup>	5-20 <sup>b</sup>
<i>Correlated</i>			
Error in excitation function of monitor reaction	3-8	3-8	3-8
Efficiency of the detector (Self-absorption, geometry)	5	5-8	12
Decay data	1	1	1
Total	8-12	10-24	16-26

<sup>a</sup>Chemical separation was done only for the  $^{45}\text{Sc}(n, p)^{45}\text{Ca}$  reaction product.

<sup>b</sup>This correction is high for low threshold reactions.

and the level density were taken as parameters to be adjusted to the experiment. The separation energies of the emitted particles were taken from Wapstra and Bos [21] or calculated using the mass excess values [11].

#### IV. RESULTS AND DISCUSSION

The experimentally determined cross sections of ( $n, 2n$ ), ( $n, p$ ), and ( $n, \alpha$ ) reactions on  $^{45}\text{Sc}$  and  $^{55}\text{Mn}$  are given in Tables III and IV, respectively. In general, the errors were in the range 8-12%. For ( $n, p$ ) and ( $n, \alpha$ ) reactions, with relatively low negative  $Q$  values (cf. Table I), the errors were larger due to several reasons: (a) at low neutron energies the cross sections are low, resulting in poor counting statistics; (b) at high neutron energies the uncertainties in background contributions are high; (c) the efficiency of the  $\beta^-$  detector has higher uncertainty. Except for a single value for the  $^{45}\text{Sc}(n, \alpha)^{42}\text{K}$  reaction at 7.9 MeV [23], all the data reported here over the neutron energy region below 12 MeV have been measured for the first time.

Our experimental data together with the literature values [22-44] are plotted as a function of neutron energy in Figs. 1-7. For the ( $n, 2n$ ) processes we show only those data which cover a relatively broad energy range. Several other data points around 14 MeV have also been reported (cf. [2]). Those values are generally in agreement with the data shown in the figures. The database for the  $^{45}\text{Sc}(n, p)^{45}\text{Ca}$ ,  $^{45}\text{Sc}(n, \alpha)^{42}\text{K}$ , and  $^{55}\text{Mn}(n, p)^{55}\text{Cr}$  reactions even in the energy region above 13 MeV is weak (cf. Figs. 3, 4, and 6).

TABLE III. Cross sections of  $^{45}\text{Sc}(n, x)$  reactions.

Mean neutron energy (MeV)	Cross section (mb)			
	$^{45}\text{Sc}(n, 2n)^{44}\text{Sc}^m$	$^{45}\text{Sc}(n, 2n)^{44}\text{Sc}^{m+g}$	$^{45}\text{Sc}(n, \alpha)^{42}\text{K}$	$^{45}\text{Sc}(n, p)^{45}\text{Ca}$
6.33±0.13			3.8±0.7	29.0±7.0
7.18±0.13			9.0±1.4	40.0±8.5
9.05±0.14			21.0±2.5	56.0±8.8
10.10±0.15			28.0±2.7	62.1±9.9
11.14±0.16			36.0±2.9	65.6±10.5
11.58±0.17		2.0±0.8	42.5±4.7	
11.97±0.18	9.0±0.9	21.0±2.6	48.0±6.7	67.5±16.8
12.40±0.18	24.0±2.1	52.0±6.1	51.5±9.8	
12.85±0.20	36.0±2.9	75.0±8.0	54.0±12.5	68.0±17.5

TABLE IV. Cross sections of  $^{55}\text{Mn}(n, x)$  reactions.

Mean neutron energy (MeV)	Cross section (mb)		
	$^{55}\text{Mn}(n, 2n)^{54}\text{Mn}$	$^{55}\text{Mn}(n, \alpha)^{52}\text{V}$	$^{55}\text{Mn}(n, p)^{55}\text{Cr}$
6.33±0.13		0.86±0.12	5.65±1.2
7.18±0.13		3.20±0.43	9.56±1.9
8.00±0.13		5.50±0.64	10.16±2.0
9.05±0.14		9.60±1.3	13.55±2.8
10.10±0.15		14.60±1.9	20.30±4.1
11.14±0.16	150±12	19.30±2.9	29.30±6.2
11.97±0.18	400±33	22.10±3.3	32.50±7.2
12.85±0.20	610±52		

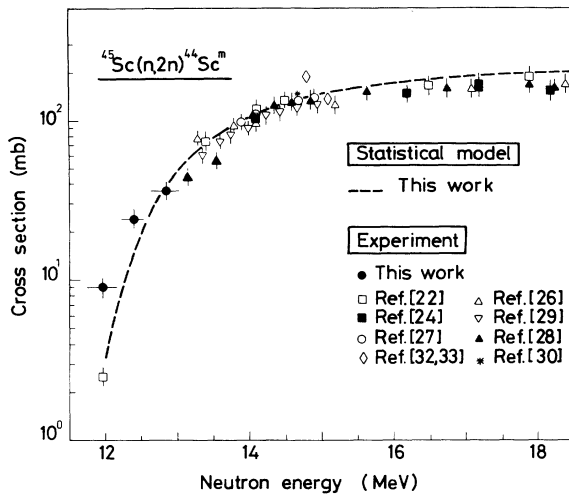


FIG. 1. Excitation function of the  $^{45}\text{Sc}(n, 2n)^{44}\text{Sc}^m$  reaction.

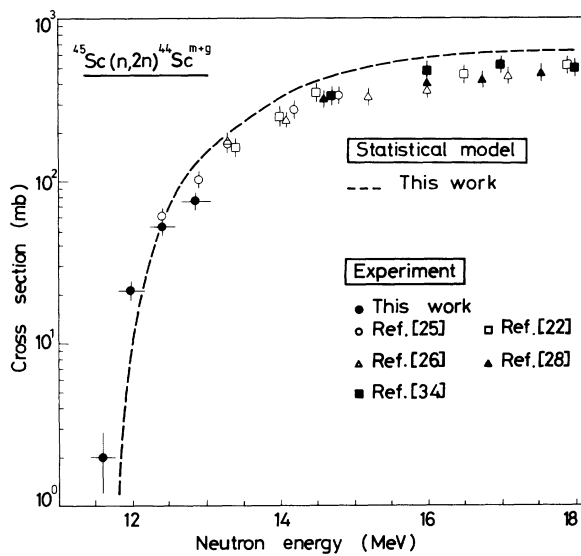


FIG. 2. Excitation function of the  $^{45}\text{Sc}(n, 2n)^{44}\text{Sc}^{m+g}$  process.

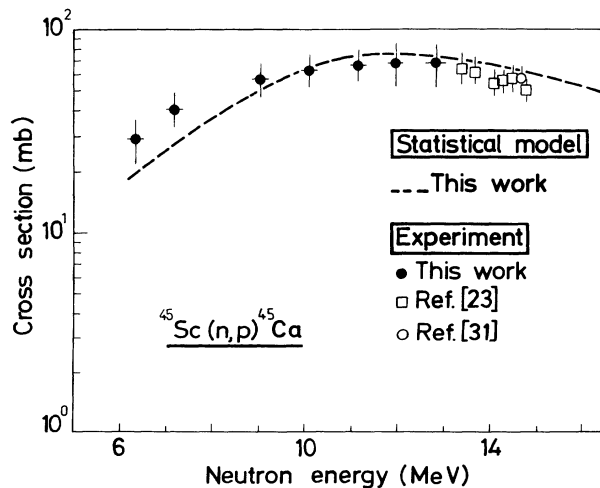


FIG. 3. Excitation function of the  $^{45}\text{Sc}(n, p)^{45}\text{Ca}$  reaction.

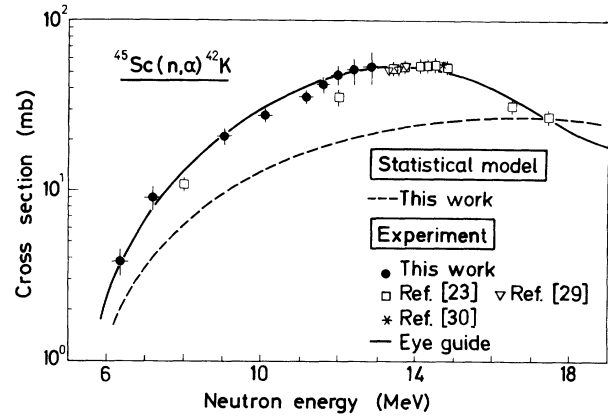


FIG. 4. Excitation function of the  $^{45}\text{Sc}(n, \alpha)^{42}\text{K}$  reaction.

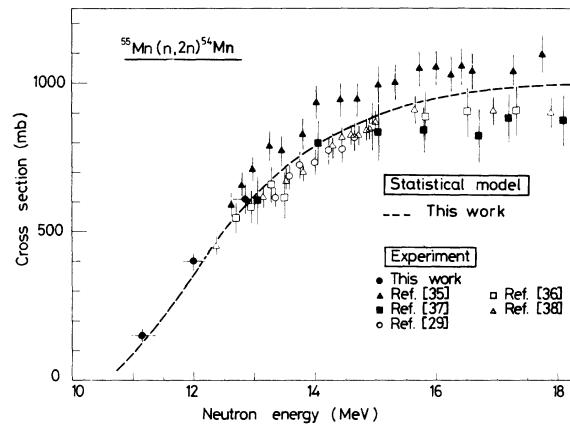


FIG. 5. Excitation function of the  $^{55}\text{Mn}(n, 2n)^{54}\text{Mn}$  reaction.

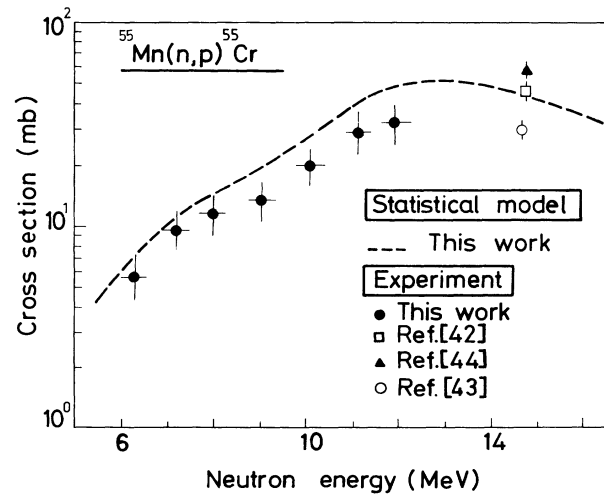


FIG. 6. Excitation function of the  $^{55}\text{Mn}(n, p)^{55}\text{Cr}$  reaction.

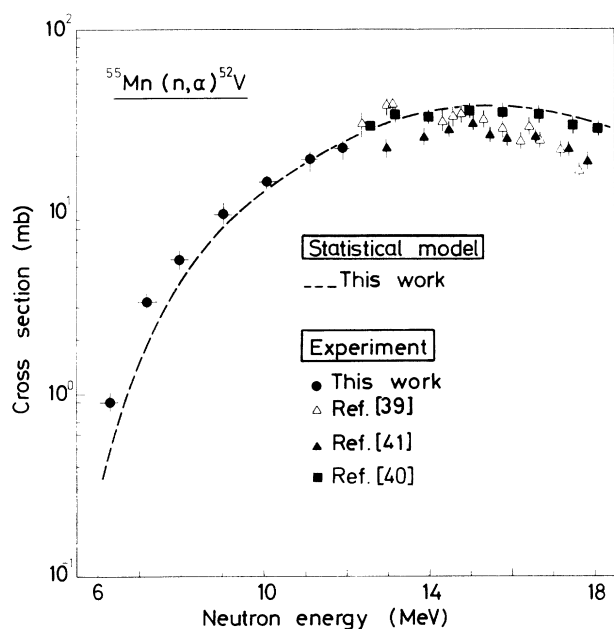


FIG. 7. Excitation function of the  $^{55}\text{Mn}(n, \alpha)^{52}\text{V}$  reaction.

A comparison of the experimental and theoretical results on the  $(n, 2n)$  reactions shows (cf. Figs. 1, 2, and 5) that, as expected, the statistical model describes this process very well, both as regards partial cross section (population of an isomeric state) and total  $(n, 2n)$  reaction cross section. Furthermore, our results confirm that the excitation function near the threshold is also reproduced well by the calculation.

The experimental excitation functions of  $(n, p)$  reac-

tions (cf. Figs. 3 and 6) appear to be reproduced reasonably well by the calculation. The calculated results for the  $^{45}\text{Sc}(n, p)^{45}\text{Ca}$  reaction depended strongly on the input information on the high-lying levels. Better agreement with experimental data was obtained when the levels above 5 MeV were neglected.

The experimental and theoretical results on the  $^{55}\text{Mn}(n, \alpha)^{52}\text{V}$  process (cf. Fig. 7) are in good agreement. For the  $^{45}\text{Sc}(n, \alpha)^{42}\text{K}$  reaction, however, the calculated cross section values are appreciably lower than the experimental data (cf. Fig. 4). A similar result was reported earlier in 14 MeV neutron induced  $\alpha$ -particle emission studies on  $^{46}\text{Ti}$  and a few other nuclei in this mass region (cf. [45,46]). Recently, the excitation functions of  $^{48}\text{Ti}(n, \alpha)^{45}\text{Ca}$  and  $^{50}\text{Ti}(n, \alpha)^{47}\text{Ca}$  reactions were investigated and the role of direct interactions was discussed [6]. The relatively low calculated  $(n, \alpha)$  values for  $^{45}\text{Sc}$  suggest that presumably for this target nucleus as well direct interactions are important. It is also somewhat surprising that the calculated  $^{45}\text{Sc}(n, \alpha)^{42}\text{K}$  excitation function does not drop beyond 14 MeV, although the  $(n, \alpha n)$  contribution was taken into account in the calculation. Evidently the present calculation cannot reproduce the  $^{45}\text{Sc}(n, \alpha)^{42}\text{K}$  excitation function well.

We thank Professor G. Stöcklin for his active support of this research program, the crew of the Compact Cyclotron CV28 for carrying out irradiations, S. Spellerberg for performing radio-chemical separations, and B. Kremer for some assistance. Some useful discussions with Dr. S. Sudár on nuclear model calculations are gratefully acknowledged. M. Bostan thanks the International Atomic Energy Agency for financial support.

- [1] CINDA-A, *The Index to Literature and Computer Files on Microscopic Neutron Data* (IAEA, Vienna, 1990).
- [2] V. McLane, C. L. Dunford, and P. F. Rose, *Neutron Cross Sections* (Academic, New York, 1988), Vol. 2.
- [3] S. M. Qaim, R. Wölfe, M. M. Rahman, and H. Ollig, *Nucl. Sci. Eng.* **88**, 143 (1984).
- [4] S. M. Qaim and R. Wölfe, *Nucl. Sci. Eng.* **96**, 52 (1987).
- [5] S. M. Qaim, M. Ibn Majah, R. Wölfe, and B. Strohmaier, *Phys. Rev. C* **42**, 363 (1990).
- [6] S. M. Qaim, M. Uhl, N. I. Molla, and H. Liskien, *Phys. Rev. C* **46**, 1398 (1992).
- [7] S. Cabral, G. Börker, H. Klein, and W. Mannhart, *Nucl. Sci. Eng.* **106**, 308 (1990).
- [8] IRDF (International Radiation Dosimetry File) (1990). Issued by the International Atomic Energy Agency, Vienna, as a computer file.
- [9] I. Birn, "NEUT" "Ein Programm zur Berechnung von Neutronenspektren erzeugt durch die  $D(d, n)^3\text{He}$ -Reaktion in einem Gastarget am Zyklotron," KFA Jülich, Internal Report No. INC-IB-1, 1992 (unpublished).
- [10] I. Birn and S. M. Qaim, *Nucl. Sci. Eng.* (to be published).
- [11] E. Browne and R. B. Firestone, *Table of Radioactive Isotopes*, edited by V. S. Shirley (Wiley, London, 1986).
- [12] M. Uhl and B. Strohmaier, Institut für Radiumforschung und Kernphysik Report No. 76/01, 1976 (unpublished) and Addenda to this report. See also B. Strohmaier and M. Uhl, International Atomic Energy Agency Report No. IAEA-SMR-43, 1980, p. 313 (unpublished).
- [13] J. Rapaport, V. Kulkarni, and R. W. Finlay, *Nucl. Phys.* **A330**, 15 (1979).
- [14] F. G. Perey and B. Buck, *Nucl. Phys.* **32**, 353 (1962).
- [15] L. McFadden and G. R. Satchler, *Nucl. Phys.* **84**, 177 (1966).
- [16] F. C. Williams, Jr., *Phys. Lett.* **31B**, 184 (1970).
- [17] C. Kalbach, *Z. Physik* **A287**, 319 (1978).
- [18] L. Milazzo-Colli and G. Braga-Marcazzan, *Nucl. Phys.* **A210**, 297 (1973).
- [19] T. W. Burrows, *Nucl. Data Sheets* **65**, 1 (1992); **40**, 149 (1983); D. E. Alburger, *ibid.* **49**, 237 (1986); Zhou Chunmei, *ibid.* **63**, 229 (1991); Zhou Chunmei, Zhou Enchen, Lu Xiane, and Huo Junde, *ibid.* **48**, 111 (1986); Huo Junde, Hu Dailing, Sun Huibin, You Janming, and Hu Baohua, *ibid.* **58**, 677 (1989); Huo Junde and Hu Dailing, *ibid.* **61**, 47 (1990); Wang Gongqing, Zhu Jiabi, and Zhang Jingen, *ibid.* **50**, 255 (1987); Huo Junde, *ibid.* **64**, 723 (1991); J. K. Tuli and R. R. Kinsey, *ibid.* **51**, 1 (1987).
- [20] W. Dilg, W. Schantl, H. Vonach, and M. Uhl, *Nucl. Phys.* **A217**, 269 (1973).
- [21] A. H. Wapstra and K. Bos, *At. Data Nucl. Data Tables* **19**, 215 (1977).
- [22] R. J. Prestwood and B. P. Bayhurst, *Phys. Rev.* **121**, 1438 (1961).
- [23] B. P. Bayhurst and R. J. Prestwood, *J. Inorg. Nucl. Chem.* **23**, 173 (1961).

- [24] B. P. Bayhurst, J. S. Gilmore, R. J. Prestwood, J. B. Wilhelm, N. Jarmie, B. H. Erkkila, and R. A. Hardekopf, *Phys. Rev. C* **12**, 451 (1975).
- [25] J. Fréhaut and G. Mosinski, in *Proceedings of the Conference on Nuclear Cross Sections and Technology*, Washington D.C. (1975), NBS Special Publication 425, US Department of Commerce, Vol. 2, p. 859.
- [26] C. G. Hudson, W. L. Alford, and S. K. Ghorai, *Ann. Nucl. Energy* **5**, 589 (1978).
- [27] D. R. Nethaway, *Nucl. Phys.* **A190**, 635 (1972).
- [28] M. Hongchang, L. Jizhou, H. Jianzhou, F. Peiguo, and L. Hanlin, *Chin. J. Nucl. Phys.* **2**, 47 (1980).
- [29] Y. Ikeda, C. Konno, K. Oishi, T. Nakamura, H. Miyade, K. Kawade, H. Yamamoto, and T. Katoh, Japan Atomic Energy Research Institute Report No. JAERI-1312, 1988 (unpublished).
- [30] R. Pepelnik, B. Anders, and B. N. Bahal, *Radiat. Eff.* **92**, 211 (1986).
- [31] J. Csikai and S. Nagy, *Nucl. Phys.* **A91**, 222 (1967).
- [32] T. H. Kao and W. L. Alford, *Nucl. Phys.* **A237**, 11 (1975).
- [33] P. K. Eapen and G. N. Salaita, *J. Inorg. Nucl. Chem.* **37**, 1121 (1975).
- [34] L. R. Veesser, E. D. Arthur, and P. G. Young, *Phys. Rev. C* **16**, 1792 (1977).
- [35] A. Paulsen and H. Liskien, *J. Nucl. Energy, Parts A/B* **19**, 107 (1965).
- [36] H. O. Menlove, K. L. Coop, H. A. Grench, and R. Sher, *Phys. Rev.* **163**, 1308 (1967).
- [37] M. Bormann and B. Lammers, *Nucl. Phys.* **A130**, 195 (1969).
- [38] L. Hanlin, L. Jizhou, F. Peiguo, and H. Jianzhou, *Chin. J. Nucl. Phys.* **2**, 286 (1980).
- [39] F. Gabbard and B. D. Kern, *Phys. Rev.* **128**, 1276 (1962).
- [40] M. Bormann, E. Fretwurst, P. Schehka, G. Wregé, H. Buttner, A. Lindner, and H. Meldner, *Nucl. Phys.* **63**, 438 (1965).
- [41] E. Zupranska, K. Rusek, J. Turkiewicz, and P. Zupranska, *Acta Physica Polonica* **B11**, 853 (1980).
- [42] R. Prasad and D. C. Sarkar, *Nuovo Cimento* **3A**, 467 (1971).
- [43] B. Minetti and A. Pasquarelli, *Z. Phys.* **199**, 275 (1967).
- [44] B. Mitra and A. M. Ghose, *Nucl. Phys.* **83**, 157 (1966).
- [45] S. M. Grimes, R. C. Haight, and J. D. Anderson, *Nucl. Sci. Eng.* **62**, 187 (1977).
- [46] R. Fischer, G. Traxler, M. Uhl, and H. Vonach, *Phys. Rev. C* **30**, 72 (1984).